Supporting information- Effect of processing conditions on the properties of vitrimerized polybutylene terephthalate prepared by reactive extrusion

Q.-A. Poutrel[1,2,*], R. Kmo[1], A. Cohadon[2], Boisse, J.[1] S. Rouzière[3], S. André[1], S. Hoppe[2], L. Farge[1]

[1]Université de Lorraine, CNRS, LEMTA, F-54000 Nancy, France

[2]Université de Lorraine, CNRS, LRGP, F-54000 Nancy, France

[3]Laboratoire de Physique des Solides, CNRS, Université Paris-Sud, Université Paris-Saclay, 91400 Orsay, France

Corresponding author:

Mail: *quentin-arthur.poutrel@univ-lorraine.fr*

Postal address: 1 rue Grandville, LRGP, 54000, Nancy

Key words: Vitrimer, continuous reactive extrusion, epoxy, process engineering

Experimental procedures – complementary information

FTIR Analysis

Zn(II) drying

Figure S1 shows the decrease of the peak between 3000 cm^{-1} and 3600cm^{-1} after drying overnight at 60°C.

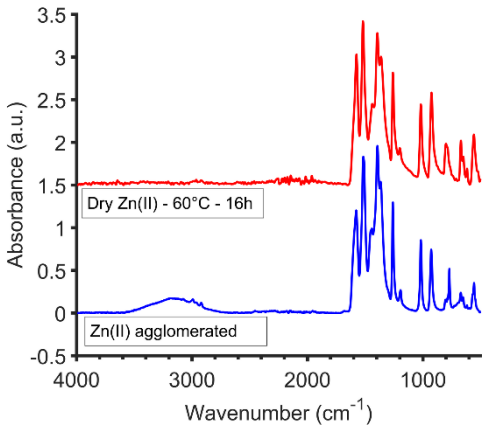

Figure S1 Zn(II) powder before and after drying at 60°C overnight

Reactive mixture (DER 332, Zn(II), Irganox 1010)

Figure S2a shows the ATR FTIR traces of the epoxy, Zn(II) catalyst, Irganox 1010, and the reactive mixture before and after dissolution. The appearance of a small peak in the 1700-1750cm^{-1} region corresponds to the Irganox 1010. Before solvation, none of the Irganox 1010 or Zn(II) can be detected on the ATR cell, as the epoxy forms a liquid layer that does not allow the detection of a solid product. These peaks were detected after dissolution. However, to exclude any possible hydrolysis of epoxy by hot water, the ratio A_{917}/A_{1505} was compared before and after dissolution. Before dissolution, the ratio was found to be ~0.43 and after dissolution, it was ~0.42. Moreover, the slight apparent decrease in the oxirane ring trace (figure S2), can be attributed to the decrease of epoxy concentration on the ATR cell once the solid products have been solvated.

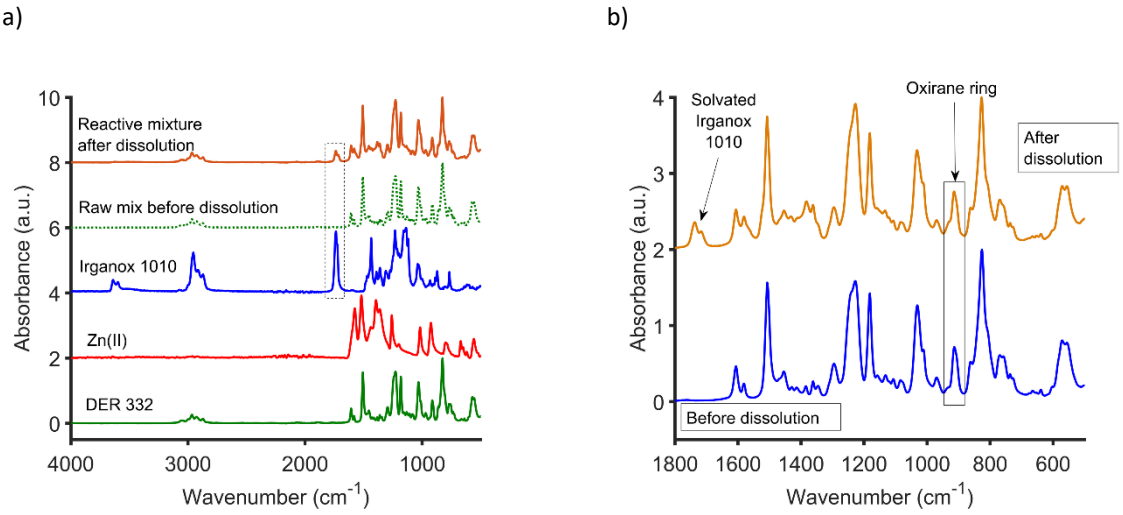

Figure S2 a) ATR-FTIR of the different products and the reactive mixture before and after dissolution, b) Reactive mixture in the 500-1800 cm^{-1} before and after dissolution.

Reactive mixing with PBT

Table S1 Operating conditions to control extrusion residence time - In this case, the residence time corresponds to the time between the injection of the epoxy+catalyst mixture and the extruder die exit.

Residence time	Screw rotation speed Rpm	Feeder rpm	t_{min}	t_{max}	t_{end}	Sample name
< 2min 30s	50	300	2min20s	2min50s	3min45	$Extru_{50}$
	100	135	2min27s	3min05	4min	$Extru_{100}$
	200	110	2min34s	3min10s	3min50	$Extru_{200}$
> 8 min	50	90	7min20s	10min00s	15min30	$Extru_{50\_long}$
	100	94	6min50s	9 min 40s	11 min	$Extru_{100\_long}$
	200	70	7min02s	8min35s	10min30	$Extru_{200\_long}$

For all experiments, t_{min} (onset of coloration or breakthrough time), t_{max} (maximum coloration), and t_{end} (end of coloration) were measured once steady-state conditions were reached (usually > 10 x t_{max}). For all extruded formulations, sampling began after t_{end} to ensure steady-state sampling of both PBT and reactive solution (epoxy and catalyst).

Table S2 Quantity of injected monomers during reactive extrusion for each formulation.

	Flow rate (g/h)				
Sample	PBT	Epoxy	$Zn_{(II)}$	Irganox 1010	Reactive mixture
$Extru_{50}$	2439.50	45.80	9.2	4.6	59.5
$Extru_{100}$	1002.40	18.80	3.8	1.9	24.5
$Extru_{200}$	784.60	14.70	2.9	1.5	19.1
$Extru_{50\_long}$	610.40	11.50	2.3	1.2	14.9
$Extru_{100\_long}$	645.30	12.10	2.4	1.2	15.7
$Extru_{200\_long}$	436.20	8.20	1.6	0.8	10.6

Dimension of tensile specimen

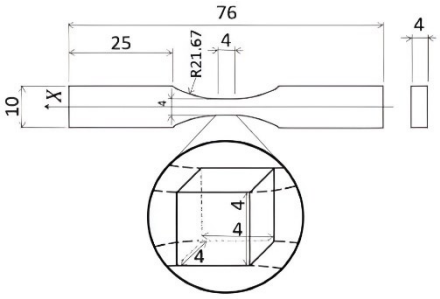

Figure S3 Dimension of the tensile specimen used in this study (mm)

Experimental results – complementary figures

Melt rheology

a)

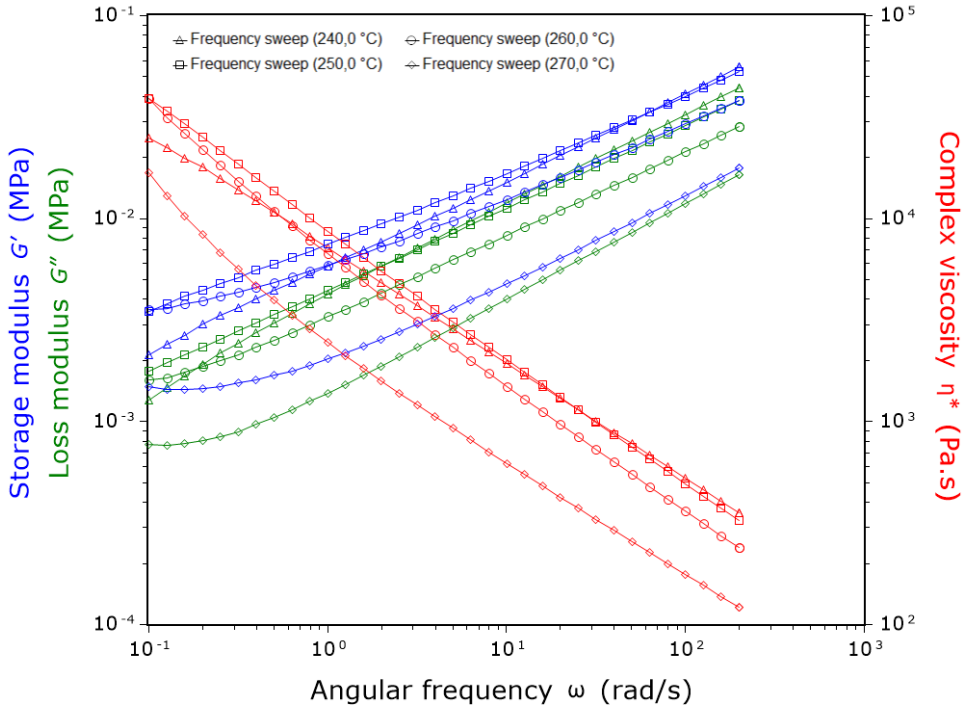
Frequency sweep (240,0 °C)
Frequency sweep (250,0 °C)
Frequency sweep (260,0 °C)
Frequency sweep (270,0 °C)
Storage modulus G′ (MPa)
Loss modulus G″ (MPa)
Complex viscosity η* (Pa.s)
Angular frequency ω (rad/s)

b)

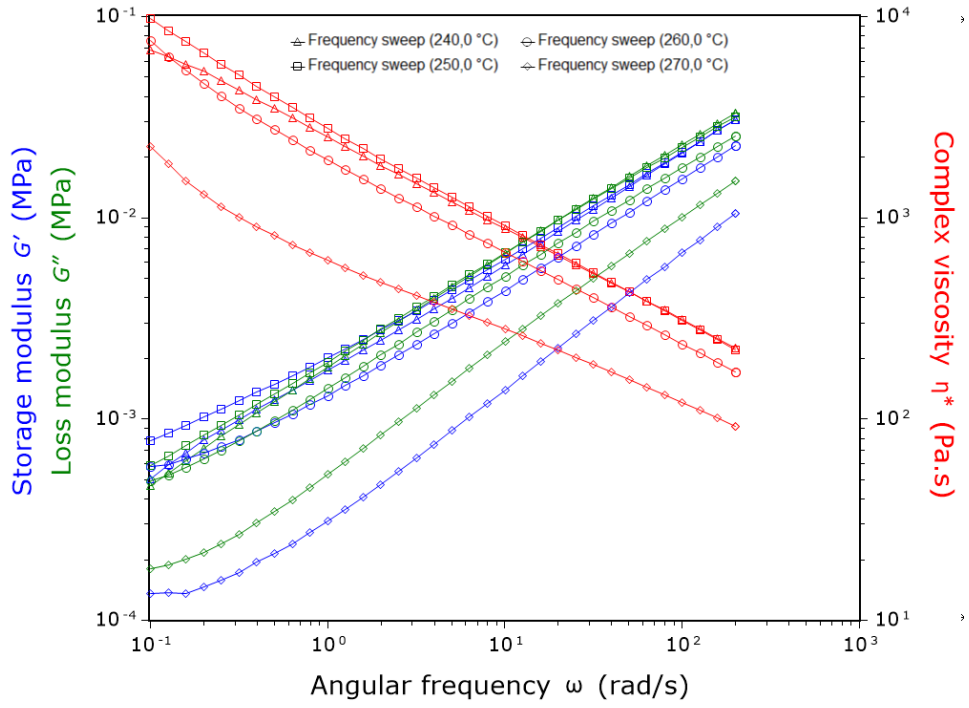
Frequency sweep (240,0 °C)
Frequency sweep (250,0 °C)
Frequency sweep (260,0 °C)
Frequency sweep (270,0 °C)
Storage modulus G′ (MPa)
Loss modulus G″ (MPa)
Complex viscosity η* (Pa.s)
Angular frequency ω (rad/s)

c)

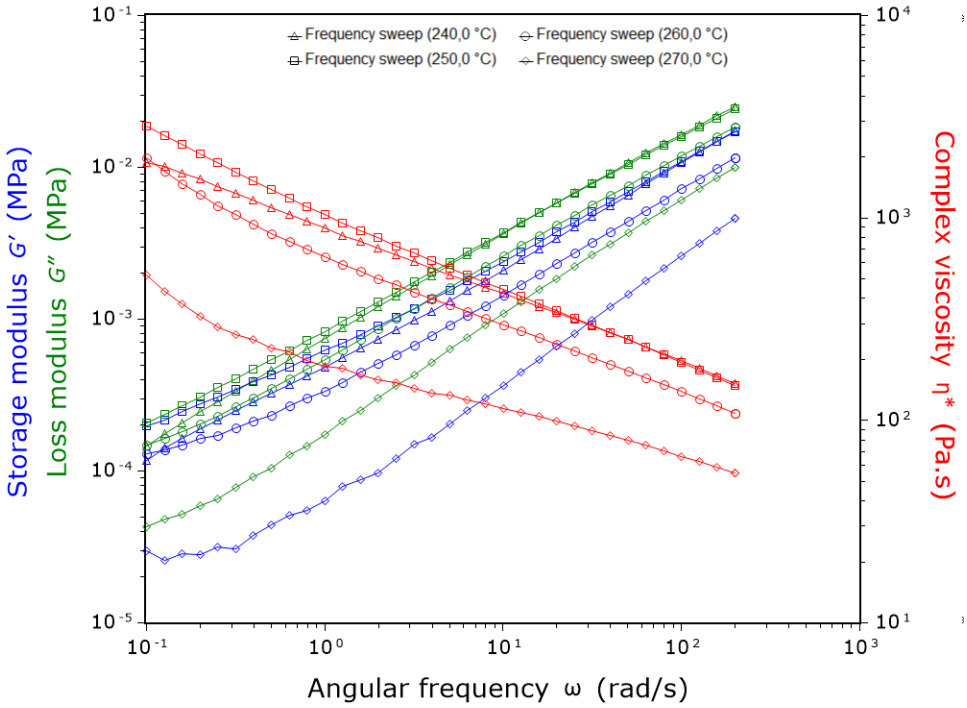
Frequency sweep (240,0 °C)
Frequency sweep (260,0 °C)
Frequency sweep (250,0 °C)
Frequency sweep (270,0 °C)
Storage modulus G′ (MPa)
Loss modulus G″ (MPa)
Complex viscosity η* (Pa.s)
Angular frequency ω (rad/s)

d)

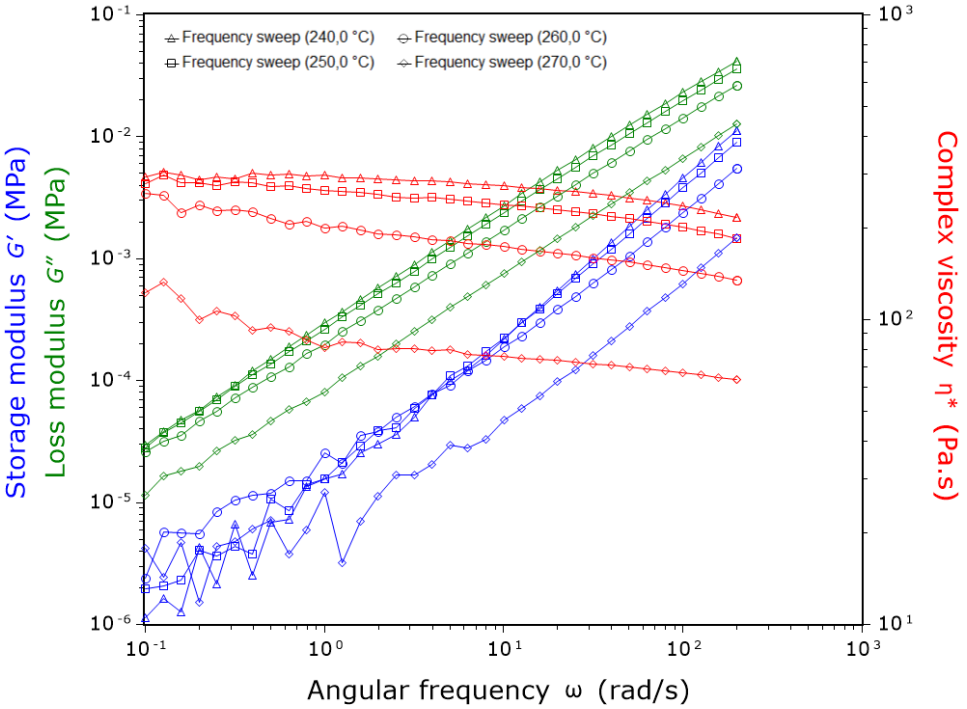
Frequency sweep (240,0 °C)
Frequency sweep (260,0 °C)
Frequency sweep (250,0 °C)
Frequency sweep (270,0 °C)
Storage modulus G′ (MPa)
Loss modulus G″ (MPa)
Complex viscosity η* (Pa.s)
Angular frequency ω (rad/s)

e)

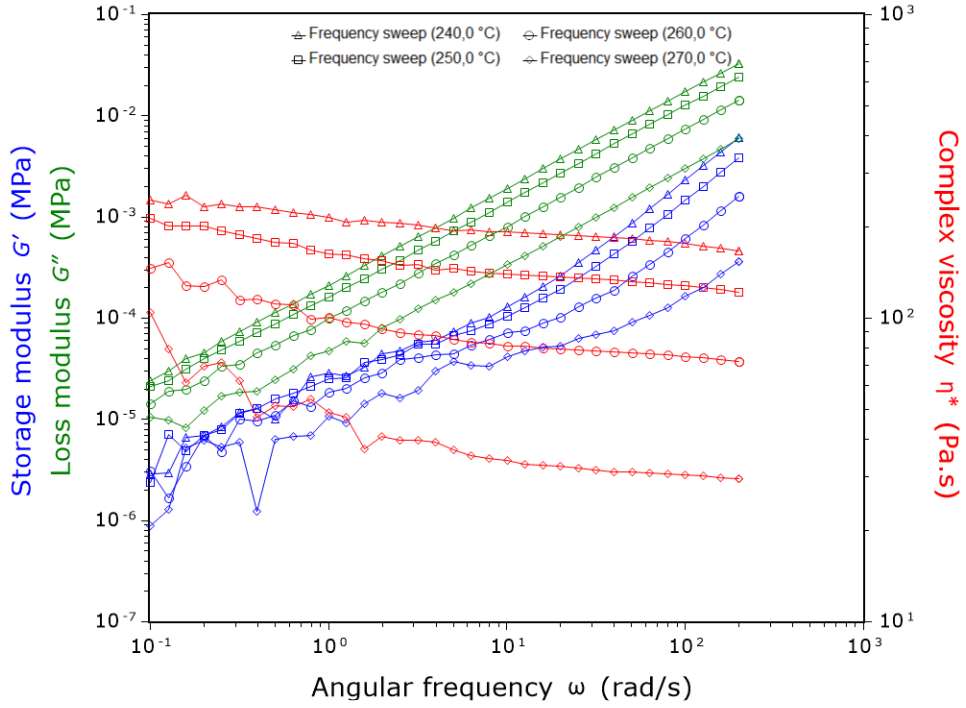

Figure S4 Raw data for angular frequency testing at different temperatures for: a) Extru_50, b) Extru_100, c) Extru_200, d) Pristine PBT, and e) Extruded PBT.

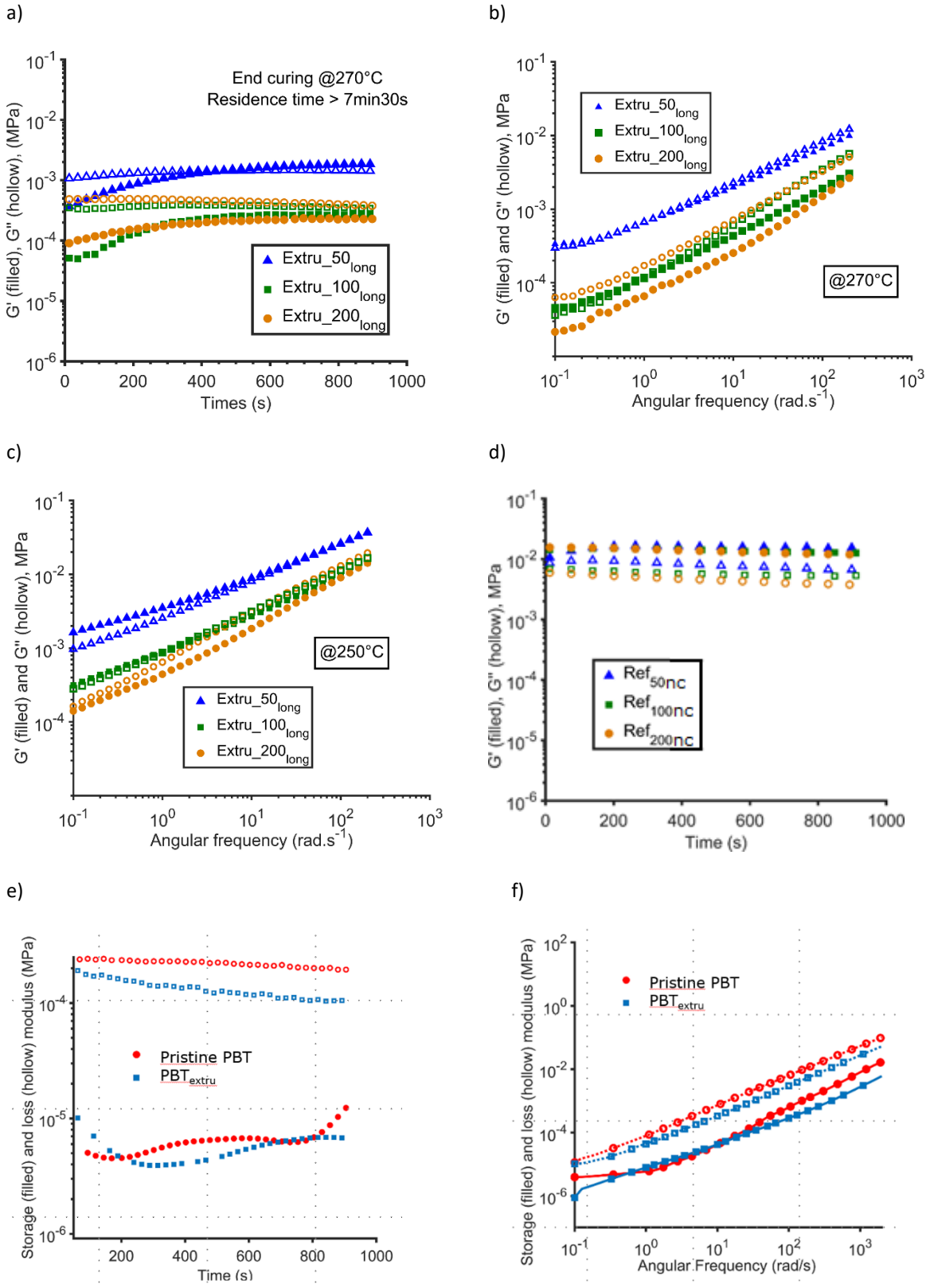

Figure S5 Complementary rheological data: a) time-sweep results for long residence time in the extruder, b) angular frequency tests performed on formulation extruded at long residence time at 270°C, c) same measurement at 250°C, d) time sweep experiment for formulation prepared in the microcompounder, e) time-sweep for Pristine PBT and PBT_{extru}, f) angular frequency test at 270°C for both PBT.

DSC

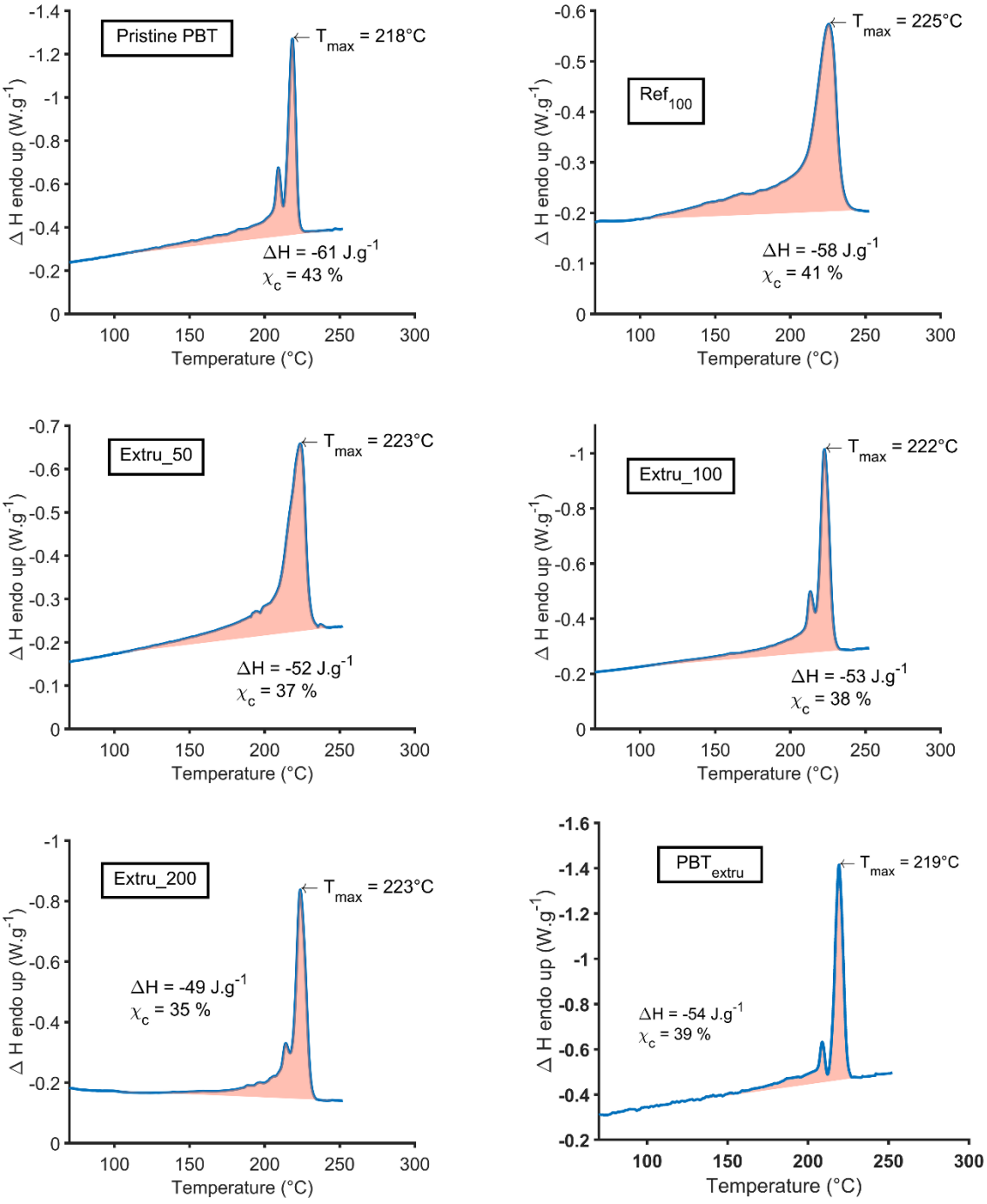

Figure S6 DSC measurements and integration of pristine PBT, Ref_{100}, Extru_50, Extru_100, and Extru_200.

Tensile testing

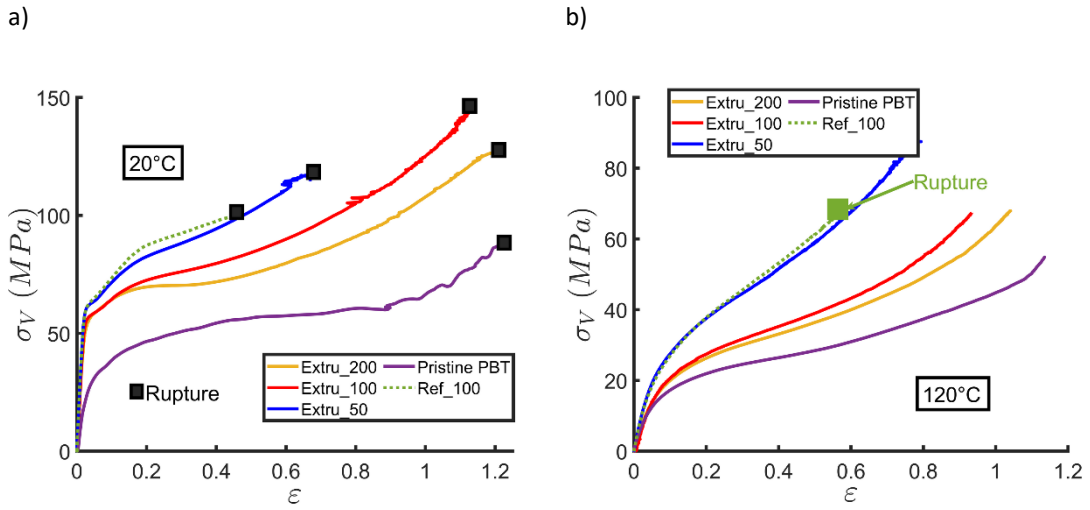

Figure S7 True stress-True strain curves A) $\sigma_v(\varepsilon)$ curves measured at room temperature, B) $\sigma_v(\varepsilon)$ curves measured at 120°C. . The Young modulus (E) was measured by fitting the curve in the $\varepsilon \in [3\ \ 9] \times 10^{-3}$ interval.

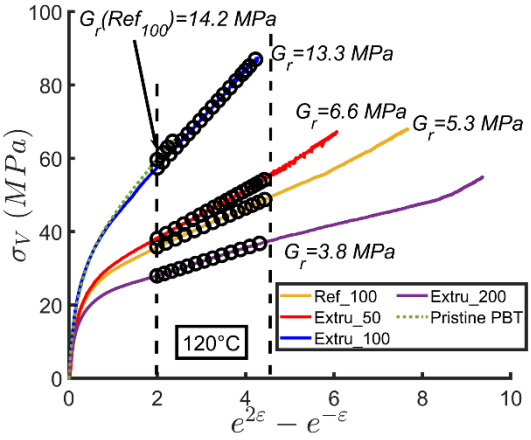

Figure S8 σ_v versus $e^{2\varepsilon} - e^{-\varepsilon}$ (Haward-Thackray representation) at 120°C. The strain hardening modulus (G_r) was measured by fitting the curve in the $e^{2\varepsilon} - e^{-\varepsilon} \in [2\ \ 4.5]$ interval. Of note, the different specimens show no or very moderate necking. Therefore, the strain rate variations are limited during the tests and the $\sigma_V(e^{2\varepsilon} - e^{-\varepsilon})$ curves exhibit good linearity in the plastic regime.

Creep

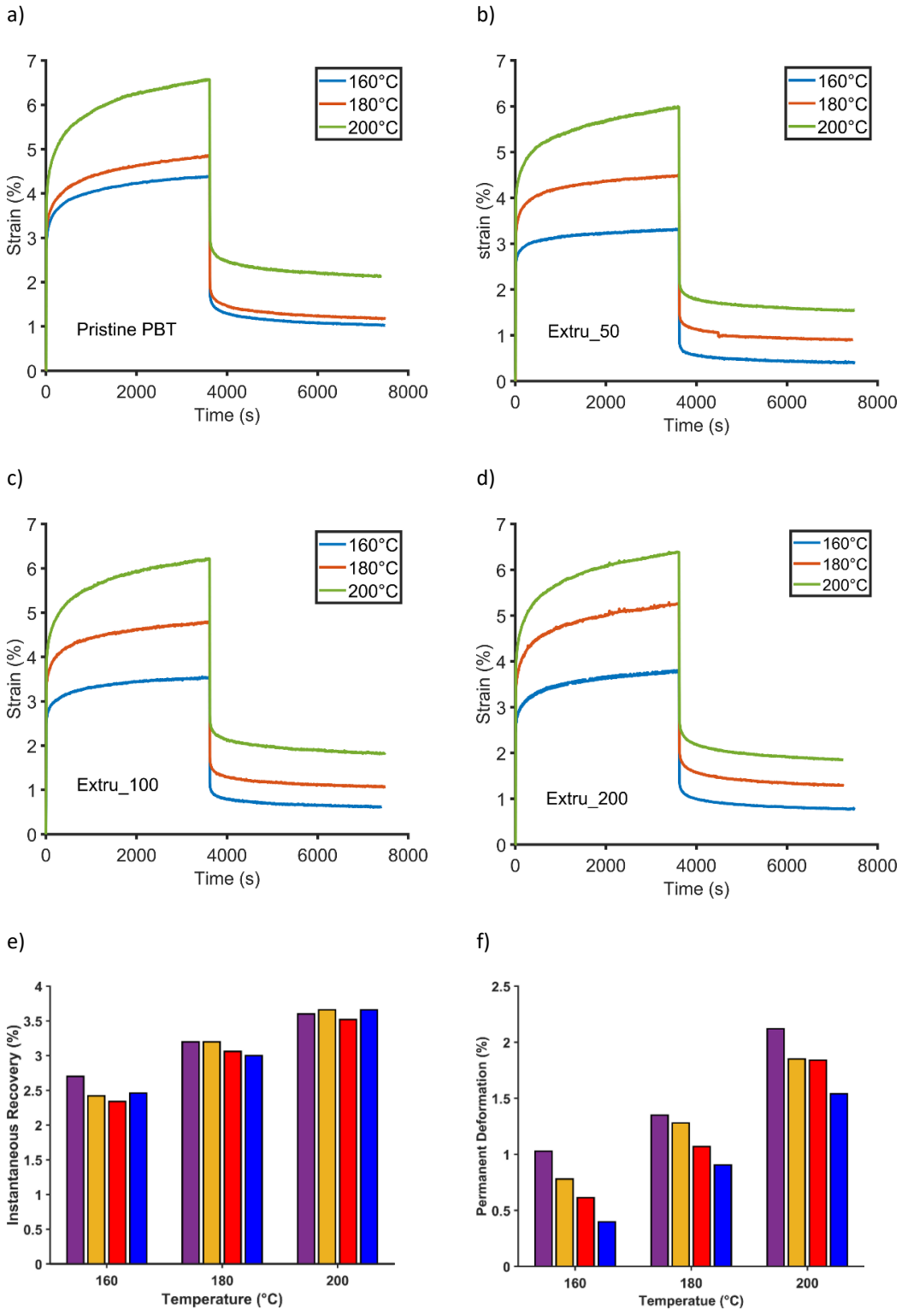

Figure S9 Creep results at 160°C, 180°C and 200°C for: a) Pristine PBT, b) Extru_50, c) Extru_100, and d) Extru_200, e) instantaneous strain recovery and f) permanent deformation.

In reference to Figure S10, the measurement of creep values is categorized into distinct phases and parameters to elucidate the material's response to stress. The "creep phase" denotes the period during which stress is applied, capturing how the material deforms under constant load. Following this, the "relaxation phase" begins upon the removal of stress, tracking the material's recovery from deformation. The "creep rate" is determined as the slope of the creep curve between 2500 seconds and 3500 seconds. The "creep strain" refers to the maximum strain observed at the end of the creep phase, indicating the extent of deformation due to the applied stress. Immediately after the cessation of stress, the "instantaneous recovery" is assessed, representing the initial strain recovery. The "time-dependent recovery" is measured during the relaxation phase, reflecting the strain that the material gradually regains over time. Finally, the "permanent deformation" is the residual deformation at the conclusion of the relaxation phase.

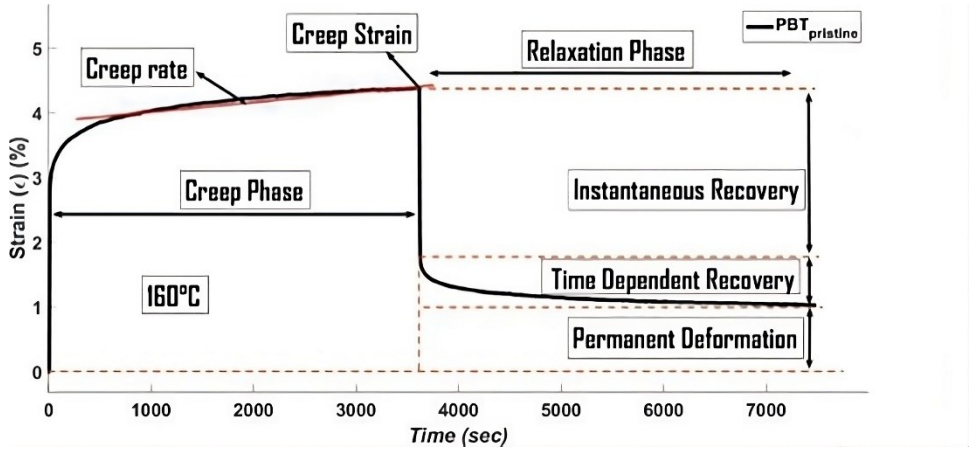

Figure S10 Schematic representing how the creep values were calculated, red line was slightly tilted on the schematic for better visibility; actual creep rate was taken between 2500s and 3500 second of the test corresponding to the secondary stage of creep for all samples

XRD – complementary results

Diffraction pattern

A)

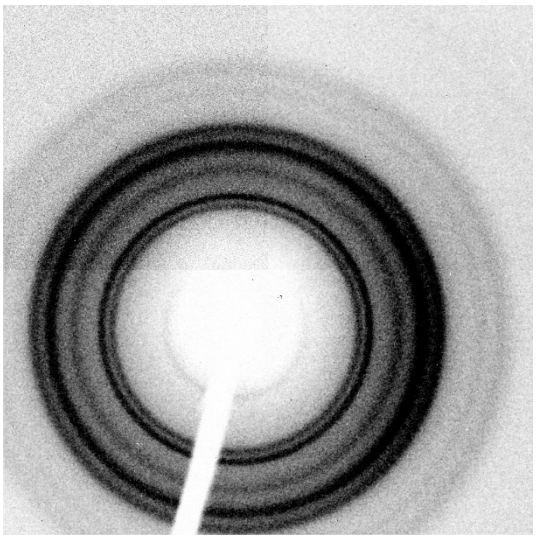

B)

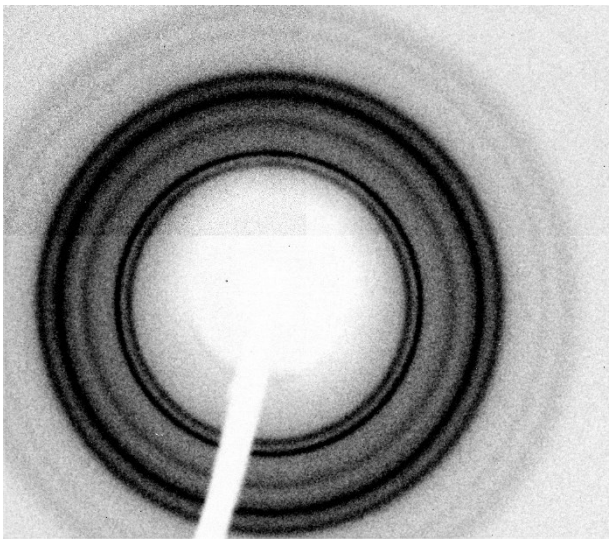

C)

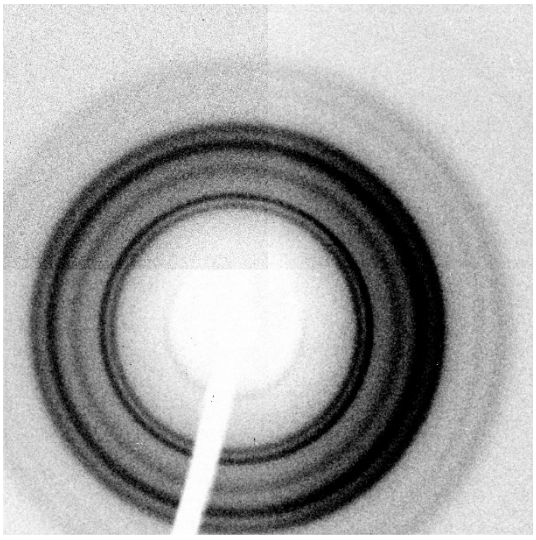

D)

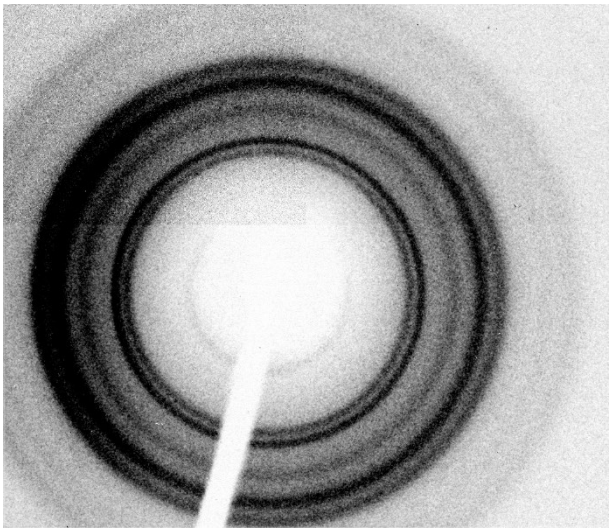

Figure S11 Diffraction pattern of samples prepared by compression molding: a) core of Extru_50, B) skin of Extru_50, C) core of Extru_100, and D) skin of Extru_100

A.3.2 Decomposition procedure

The aim of decomposition is to extract individual contributions of each peak from the overall signal. The deconvolution procedure was performed on intensity profiles $I(2\theta)$ taken along the equatorial axis. After subtraction of incoherent scattering, for each $I(2\theta)$ profile a parabolic background was fitted to the limits of the interval $2\theta \in [14° 28°]$ and subtracted from the profile. We do not believe that it is problematic since the

assessment of crystal size is done for comparative purposes only. The obtained radial Intensity profiles were then approximated by a sum of several Pearson VII functions.[1] Each Pearson VII was associated to a given peak. The Pearson VII function has the form:

$$f(2\theta) = \frac{A}{\left[1 + 4\left(\frac{2\theta - 2\theta_{hkl}}{\Delta(2\theta_{hkl})}\right)^2 \left(2^{\frac{1}{m}} - 1\right)\right]^m}$$

θ_{hkl} is the Bragg angle for the crystallographic reflections. Its determination was not part of the fitting procedure in this study. It was calculated using the unit cell parameters of the PBT α form published by Huo et al.[2](see table S3). It was checked that the peak positions remain the same for the neat PBT, Extru_50 and Extru_100 (see Figure S13). The fitted parameters characterising the peak shapes are A, m and $\Delta(2\theta_{hkl})$ for each peak. A is the height of the peak. $\Delta(2\theta_{hkl})$ is the full width at half maximum. m is the shape parameter of the function, which can be interpreted as follows: when $m = 1$, the Pearson VII distribution is reduced to the Cauchy function, and when $m \to \infty$, the Pearson VII takes the Gaussian form.

In the case of PBT, in the $2\theta \in [14° \; 28°]$ range of our study, 10 bands or envelopes were expected. Associated Miller indices and peak positions are resumed in table S3.

Table S3 Miller indices (hkl), lattice spacings (d_{hkl}) and positions ($2\theta_{hkl}$) of the 10 peaks present in the $2\theta \in [14° \; 28°]$ range. θ_{hkl} and d_{hkl} are of course related by the Bragg equation ($\lambda = 2d_{hkl}sin\theta_{hkl}, with \; \lambda = 1.54$ Å). The lattice spacings were first calculated using the unit cell parameters of the α PBT form given by Huo et al. for T=20°C.

$\boldsymbol{hkl}$	$\mathbf{01\bar{1}}$	**010**	**002**	$\mathbf{\bar{1}11}$	$\mathbf{1\bar{1}0}$	**011**	**100**	$\mathbf{\bar{1}12}$	$\mathbf{10\bar{3}}$	$\mathbf{1\bar{1}1}$
$\boldsymbol{d_{hkl}}$ (Å)	5.5	5.1	4.8	4.3	4.2	3.9	3.8	3.7	3.6	3.5
$\boldsymbol{2\theta_{hkl}}$ (°)	16.0	17.3	18.4	20.5	21.1	22.6	23.4	24.1	24.9	25.2

The peak decomposition was carried out from the raw signal using a home-made MATLAB code. Several trials on a given set of diffraction data were performed to find the optimum peak parameters corresponding to the

[1] Selvaraj, M.; Venkatachalapathy, V.; Mayandi, J.; Karazhanov, S.; Pearce, J. M. Preparation of Meta-Stable Phases of Barium Titanate by Sol-Hydrothermal Method. AIP Adv. 2015, 5 (11). https://doi.org/10.1063/1.4935645.

[2] Huo et al. (1992). *Journal of Polymer Science Part B: Polymer Physics*, *30*(13), 1459-1468

minimum relative error between the fitted curve (red curve in Fig S12) and the experimental curve (black curve in Fig. 1). In Figure 1, we also show the individual contributions of each peak determined through our procedure. Peaks with Miller indices [010] and [100] (peaks used for the analysis in the paper) are highlighted in green. In Figure S13, we also show the individual contributions of each peak determined through our procedure.

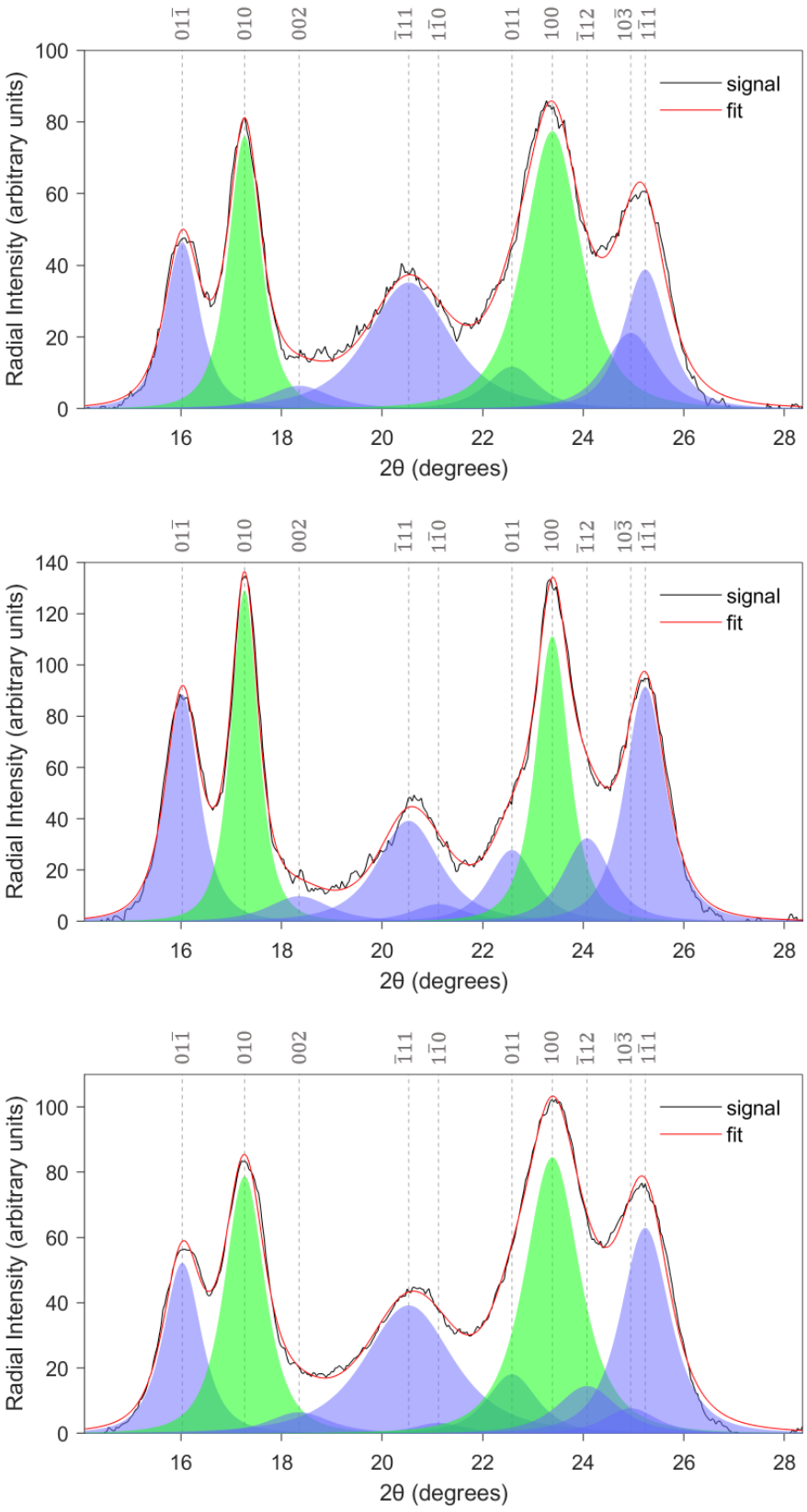

Figure S12 Radial intensity signal (grey curves) taken along the direction φ=0° and fit (red curves) for Pristine PBT, Extru_50 and Extru_100 sample (from top to bottom)

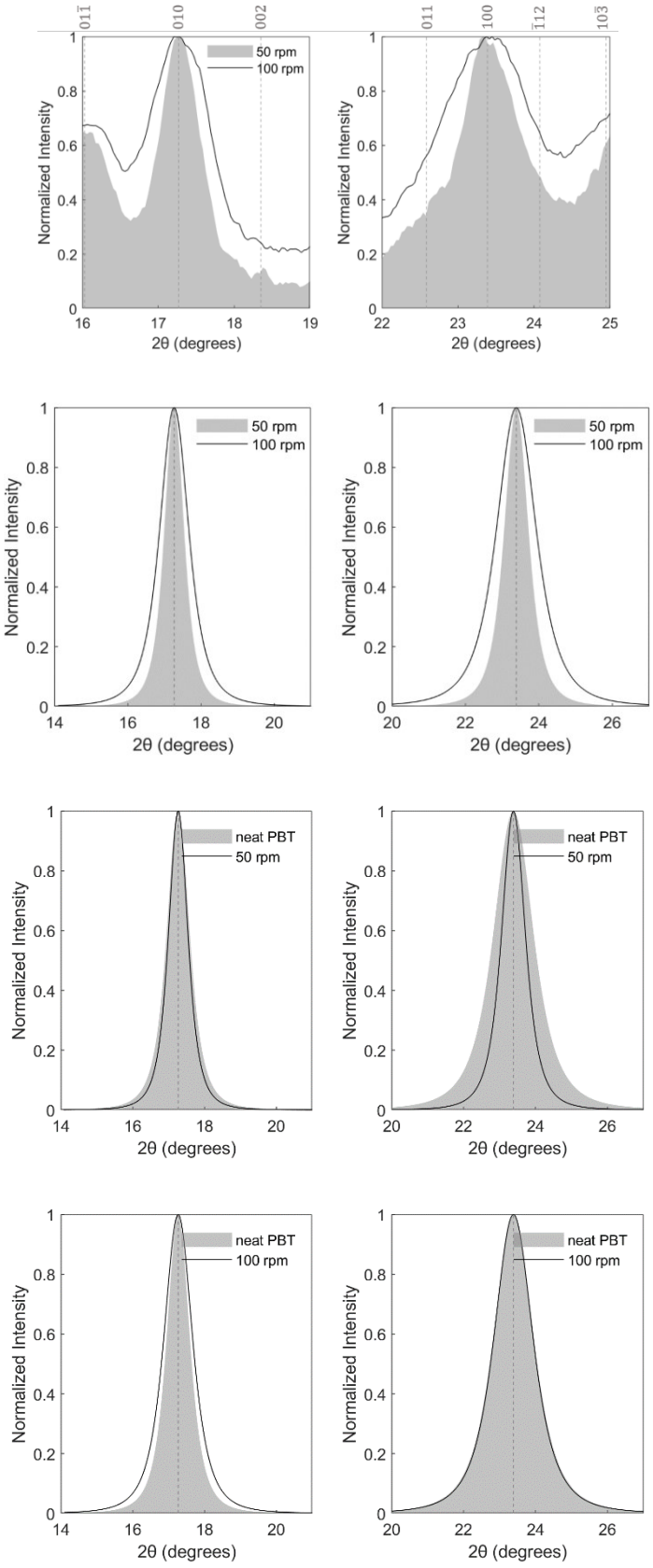

Figure S13Pics enlargement from Extru_50 to Extru_100 samples and compared to PBT for each samples: raw signals (top) and peak fits (bottom) normalized by the maximum values of peaks with Miller indices (010) (left) and (100) (right).

Discussion – complementary figures

Calculation of energy activation

The real viscosity was calculated using the equation $r = \frac{\sigma}{\eta}$ where r is the creep rate of the sample at different temperature, η the sample viscosity and σ is the applied stress. Then the log of viscosity was plotted versus 1000/T with T the temperature in kelvin. The slope of the resulting curves allows to obtain the activation energy of the sample.

Printing of Extru_100

a)

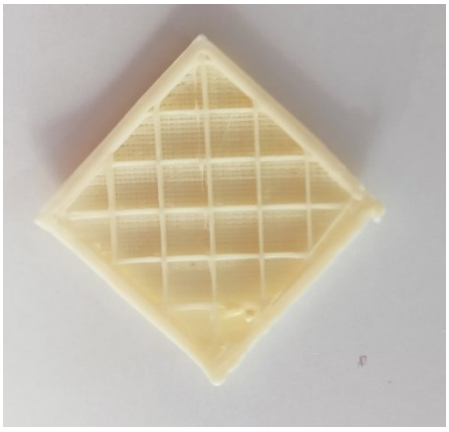

b)

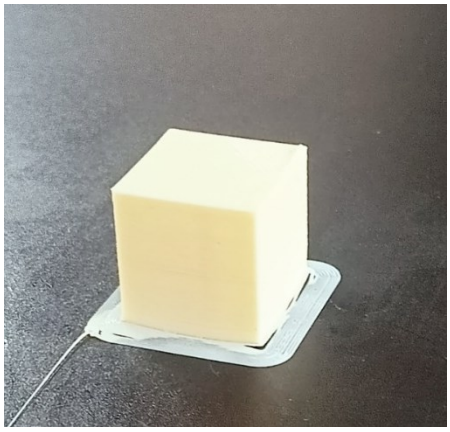

c)

d)

Figure S14 Printing of complex shapes of Extru_100 formulation: A) interior of cube pattern, B) Cube, C) Unidirectional printed tensile specimen, D) Gyroid structure.